

Deposit Formation on Fuel Cladding in PWR Primary Systems

Author

Jim Henshaw
Reading, Berkshire, UK



A.N.T. INTERNATIONAL®

© May 2022

Advanced Nuclear Technology International
Spinnerivägen 1, Mellersta Fabriken plan 4,
448 50 Tollerød, Sweden

info@antinternational.com

www.antinternational.com

Disclaimer

The information presented in this report has been compiled and analysed by Advanced Nuclear Technology International Europe AB (ANT International®) and its subcontractors. ANT International has exercised due diligence in this work, but does not warrant the accuracy or completeness of the information. ANT International does not assume any responsibility for any consequences as a result of the use of the information for any party, except a warranty for reasonable technical skill, which is limited to the amount paid for this report.

Quality-checked and authorized by:

A handwritten signature in black ink, appearing to read 'Peter Rudling', is centered below the text 'Quality-checked and authorized by:'. The signature is fluid and cursive.

Mr. Peter Rudling, Chairman of the Board of ANT International

Contents

1	Introduction	1-1
2	Historical Occurrences of PWR Fuel Crud	2-1
	2.1 Early Crud Experiences at PWR Plants.	2-1
	2.2 More Recent Crud Experiences at PWR Plants.	2-3
	2.3 Crud Induced Power Shifts (CIPS) and High Duty Cores.	2-4
3	Mechanism of Crud Formation In PWR Systems	3-1
	3.1 Overall Description of Fuel Crud Mechanism	3-1
	3.2 General Corrosion and Release from Steel and Inconel Alloys	3-5
	3.2.1 Corrosion Mechanism	3-5
	3.2.2 Effect of Temperature, pH and O ₂ concentration on Stain-less Steel Corrosion	3-7
	3.2.3 Corrosion Rates of Ni Based Alloys	3-11
	3.2.4 Corrosion Product Release	3-13
	3.3 Fuel Crud Deposition Mechanisms	3-14
	3.3.1 Dry Out/Flashing Deposition Mechanism	3-15
	3.3.2 Electrokinetic Deposition Mechanism for Fuel Crud Formation	3-15
	3.3.3 Salt Precipitation Deposition Mechanism	3-16
	3.3.4 Particle Deposition Mechanism	3-17
4	Fuel Crud Thermal Hydraulics, Properties and Chemistry	4-1
	4.1 Fuel Crud Thermal Hydraulics and Material Transport	4-1
	4.2 Chemistry Taking Place Within Fuel Crud	4-5
	4.3 Fuel Crud Properties	4-7
	4.4 Results of Fuel Crud Calculations	4-8
5	Modelling of material transport in a PWR primary circuit.	5-1
	5.1 Outline of Material Transport Models.	5-1
	5.2 Results of Material Transport Modelling.	5-4
6	Discussion and Summary	6-1
	References	
	Unit conversion	

1 Introduction

Formation of deposits on Pressurised Water Reactor (PWR) fuel cladding has been an inherent problem in these systems since their inception [Odar, 2014] and remains a problem to-date [Kim et al, 2021; Yeon et al, 2010; Maeng et al, 2008]. How these deposits arise, their structure, composition and what mitigating strategies can be utilised to deal with them will be discussed in detail in this report. Needless to say, though, that understanding this phenomenon is difficult as it is a consequence of many interacting physical processes including: material property behaviour, coolant chemistry, thermal hydraulics (both bulk and local) and neutronics. Consequently, some understanding of each of these topics is required to appreciate the observed complex behaviour and is why, even after 5 to 6 decades of study, the nuclear industry is still tackling this problem. However, a great deal of knowledge and understanding has been gained over this period and this report will attempt to discuss some of the most useful studies that have been carried out.

The term crud is used to describe deposits on fuel clad and is thought to have arisen as the acronym for, Chalk River Unidentified Deposit, identified in early studies performed on the NRX Canadian test reactor* [Urbanic et al, 1979]. Since these early studies fuel crud has been identified in many light water cooled reactors [Sawochka et al, 1997; Byers et al, 2004; Ries, 2004] and has led to problems such as [Odar, 2014]:

- Increased pressure drops across the core [Sandberg, 1967];
- Changes in core reactivity as a consequence of increased fuel temperatures [Weisman & Bartnoff, 1965];
- Crud induced power shifts (CIPS) from the top to the bottom of the core, formally referred to as axial offset anomaly's (AOA) [Deshon, 2004];
- Fuel clad failure and fission product release [Mitchell, 1997, 1998];
- Increased levels of radioactivity at shutdown and during normal operations.

Some of these historical observations will be discussed below along with the detailed mechanism for crud formation. In summary, fuel crud arises from deposits of metal/metal oxide phases released during corrosion of out-of-core alloy surfaces. The fact that the composition, amount and distribution of crud in the core varies from reactor to reactor and often from cycle to cycle for a specific reactor [Byers et al, 2004] indicates several system variables are important in determining crud behavior. Clearly the release and deposition processes must differ from reactor to reactor and cycle to cycle, so understanding what causes these differences is essential to understanding reactor observations of fuel crud. This report will discuss the deposition and release mechanisms in great detail to attempt to correlate reactor design and operations with observed fuel crud behaviour.

Section 2 will provide a brief history of fuel crud in PWR systems. Almost all reactors during their operational life will have encountered fuel crud deposits, but it is not the intention here to provide a complete historical review of all these incidents. If the reader is interested in more historical data then it is recommended, they read [Odar, 2014]. This report will focus on the more important observations and studies which have influenced our understanding of this phenomena. The mechanisms for material release, transport and deposition in the core will be discussed in detail in Section 3. How these are influenced by material choice, coolant chemistry and core design will also be discussed. Section 4 will discuss what occurs within fuel crud that may affect its deposition rate, its effect on core neutronics and possible impact on clad corrosion leading to failure. Finally, a discussion will be given summarizing our current understanding and where future work is required to further this knowledge.

* Built in 1947, a 10-50 MW thermal, heavy water reactor.

2 Historical Occurrences of PWR Fuel Crud

2.1 Early Crud Experiences at PWR Plants.

Solomon and Roesmer [Solomon, 1976] reported fuel crud deposits found at the Point Beach and Beznau reactors during cycles 1-3. The deposits were small, with most occurring in the first cycle of operation. At Beznau 35 assemblies with fuel crud were inspected which showed a range of depositions, as shown in (Table 2-1).

Table 2-1: Reported crud deposit amounts at Beznau PWR plant [Solomon, 1976]

Grid Level	Bundle Deposits, mg/dm ²					
	A-11	A-29	A-05	B-65	B-59	C-115 C-83 C-89
6-7 (top)	64	180	204	183	223	235
5-6	--	3	--	--	--	--
Core Center -----> Periphery						

For cycle 1 the crud thickness ranged from 2-15µm (assuming a crud density of 3g/cm³), while crud thicknesses in subsequent cycles were of the order of a factor of 10 smaller. There was some indication that the amount of crud increased towards the top of the assemblies and towards the periphery of the core.

At Point Beach a range of patterns were noted for the crud distributions, as illustrated in (Figure 2-1), with a median crud amount of 46mg/dm² (~1.5µm), with slightly more deposition towards the top of the core.

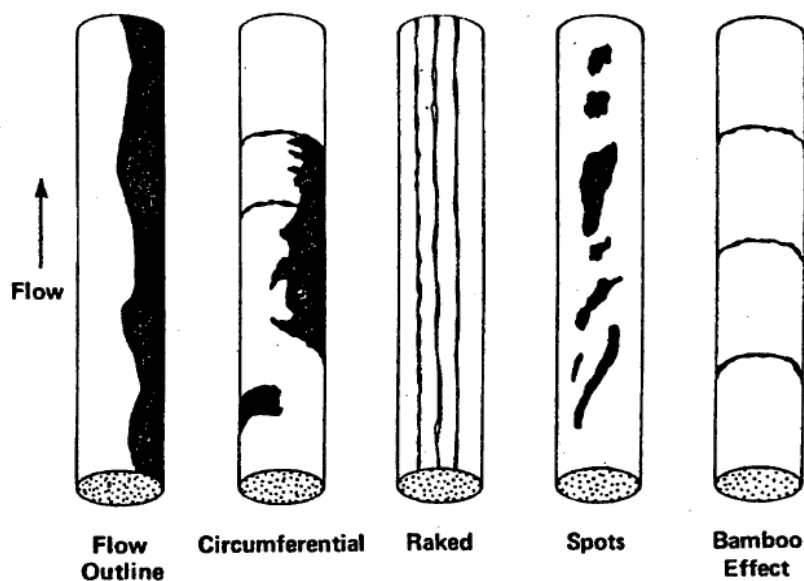


Figure 2-1: Crud distributions observed at Point Beach [Solomon, 1976].

Chemical analysis (ICP-MS) was performed on samples of the crud and results of these are shown in (Table 2-2).

3 Mechanism of Crud Formation In PWR Systems

3.1 Overall Description of Fuel Crud Mechanism

Crud on fuel cladding is a consequence of release of metals from corroding out-of-core materials into the coolant that subsequently deposit on the fuel clad. (Figure 3-1), taken from [Odar, 2014], gives a schematic representation of the processes that are occurring in the reactor:

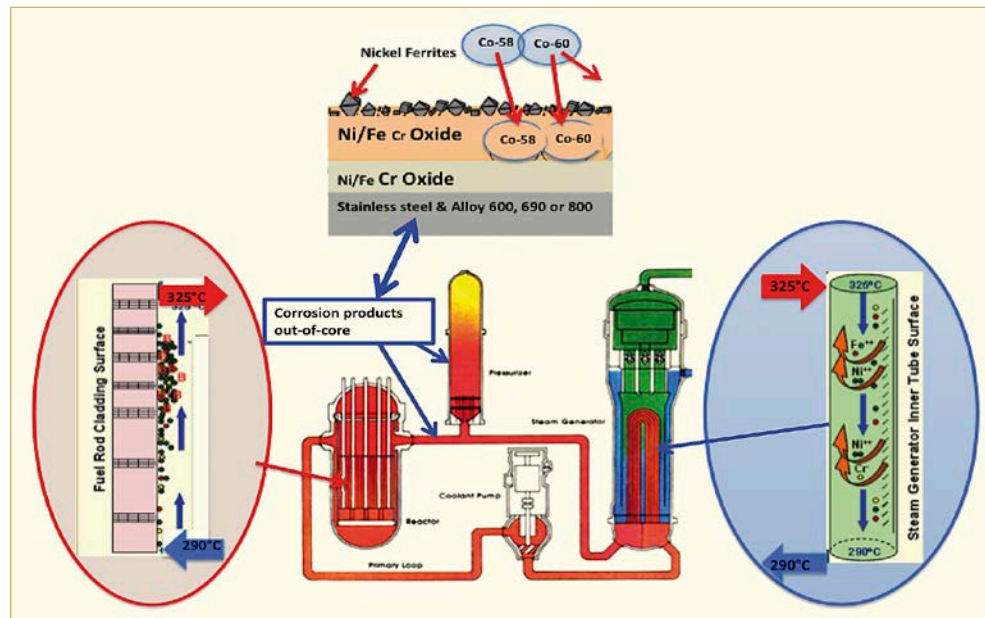


Figure 3-1: Schematic of PWR plant fuel cladding deposit formation (Odar 2014).

In Western PWR's the out-of-core systems are constructed of stainless steels (hot leg, cold leg etc) and nickel-based alloys (steam generator tubes) and so predominantly release Fe and Ni into the coolant that subsequently deposits on the fuel. In the coolant the both soluble and particulate material exists and both potentially may deposit on the clad. In general, the steam generator tubes provide the largest surface area in contact with the coolant and so it is thought this part of the primary system provides that largest quantity of material depositing in the core. However, such simple considerations should be treated with caution, (Table 3-1), taken from [Polley and Pick, 1986] shows the areas for the various materials in a 4-loop Westinghouse PWR. The ratio of Inconel SG materials area to the stainless steels surface area is approximately 7, which means that if stainless steel materials in these systems corroded roughly 7 times faster than Inconel materials then the contributions of both materials to corrosion products in the water would be roughly equivalent. That is, factors other than simple geometric considerations need to be considered when assessing the sources of fuel crud.

Table 3-1: Typical system values for a 4-loop Westinghouse PWR [Polley and Pick, 1986].

Surface Area (m ²)	Zircaloy	7x10 ³
	Inconel	1.8x10 ⁴
	Stainless Steel	2.7x10 ³
Primary System Volume (m ³)		240
CVCS Flow Rate (kg/s)		4.7
CVCS Removal Efficiency		0.9

The study by Polley and Pick also provided some early data on the composition of fuel crud, as well as the levels of Fe and Ni in the coolant. (Table 3-2) is taken from their paper

4 Fuel Crud Thermal Hydraulics, Properties and Chemistry

4.1 Fuel Crud Thermal Hydraulics and Material Transport

(Figure 4-1) is an SEM image of a piece of fuel crud from the Vogtle plant generated during cycle 8.

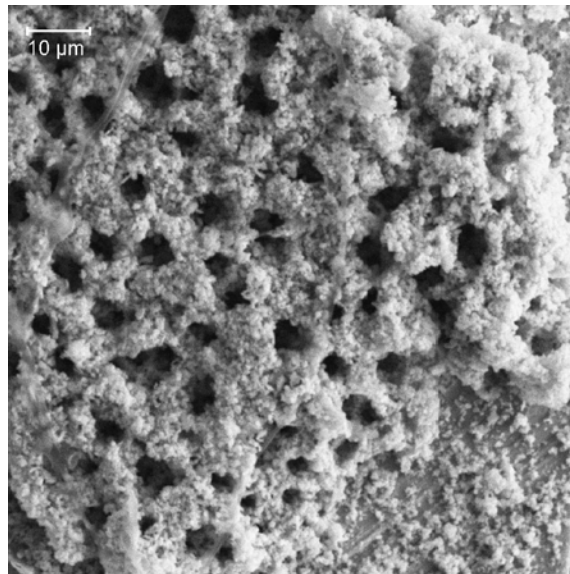


Figure 4-1: High magnification SEM of a crud flake obtained from Span 6B from Vogtle-2 Cycle 8. [Deshon, 2004].

The figure shows a typical porous material containing a number of large channels, some as large as $10\mu\text{m}$ in diameter in this figure, often referred to as steam chimneys. This structure indicated the mechanism for heat transport through the crud, first suggested by [Cohen, 1974], in which water is drawn into the crud through the crud porous matrix (shell) and exits as steam along the chimney's shown in the above figure. This heat removal mechanism is known as wick boiling. (Figure 4-2) is a schematic of a single crud chimney and surrounding porous shell, in which the total heat flux, q , from the fuel pin must be removed by conduction (q_c) and evaporation (q_v) through the crud. The Cohen model assumes zero convective heat removal within the shell because of the restraints on free fluid flow imposed by the porous medium.

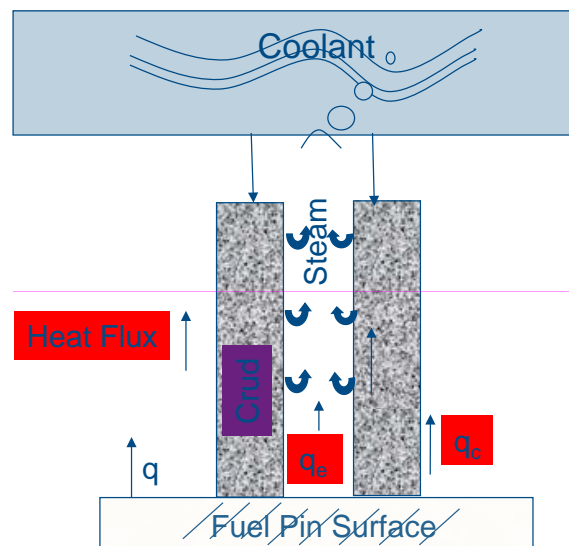


Figure 4-2: Schematic of heat transport processes through fuel crud.

Steady state heat balance between evaporation and conduction means that:

$$\text{Equation 4-1:} \quad \int_{shell} q_c dA + \int_{chimney} q_e dA = 0$$

Here the conductive heat flow is across the area parallel to the clad surface and the evaporative heat flux is along the area of the steam chimney wall. Using Gauss's divergence theorem to convert the first integral into a volume integral we can therefore write:

$$\text{Equation 4-2:} \quad \int_{shell} \frac{dq_c}{dx} dV + \int_{chimney} q_e dA = 0$$

Since the area of the chimney, $dA = 2\pi r_c dx$ and the volume of the shell $dV = f dx / N_c$, where r_c is the radius of the chimney, N_c the chimney density (number per unit area) and f the fraction of area covered by the shell ($f = 1 - N_c \pi r_c^2$), it is possible to write

$$\text{Equation 4-3:} \quad \frac{dq_c}{dx} + \frac{2\pi r_c N_c}{f} q_e = 0$$

In terms of temperature in the crud the conductive heat flux is $q_c = -k_c dT/dx$ and the evaporative heat flux is given by $q_e = h_e(T - T_s)$, where k_c is the conductivity of the crud, h_e is the evaporative heat transfer coefficient and T_s the saturation temperature of water. This leads to Cohen's equation for the temperature distribution in the crud, which is:

$$\text{Equation 4-4:} \quad \frac{d^2 T}{dx^2} - \frac{2\pi r_c N_c h_e}{f k_c} (T - T_s) = 0$$

This was originally solved by Cohen with the boundary conditions:

$$\text{Equation 4-5:} \quad T = T_o \quad \text{at } x = 0$$

$$\text{Equation 4-6:} \quad k_c \left(\frac{\partial T}{\partial x} \right)_{x=d} = \frac{q_o}{f} \quad \text{at } x = d$$

Here T_o is the temperature at the crud-coolant interface ($x = 0$) and q_o the total heat flux from the clad into the crud of thickness d . Although the boundary condition (Equation 4-5) is correct, in order to determine the temperature at the crud-water interface it is necessary to apply the boundary condition:

$$\text{Equation 4-7:} \quad k_c \left(\frac{\partial T}{\partial x} \right)_{x=0} = h_{fc} (T_b - T_o)$$

Here T_b is the bulk coolant temperature and h_{fc} is the forced convection heat transfer coefficient in the presence of boiling, note this is different than the forced convection term with no boiling e.g., using a Dittus-Boulter correlation [Collier & Thome, 1994].

Mass balance through the crud means that the mass of water flowing into the shell must equal the mass of steam exiting from the chimney. Analogous to the equation for heat balance it is possible to express mass conservation as:

$$\text{Equation 4-8:} \quad \int_{shell} \rho_w u_l dA + \int_{chimney} j_e dA = 0$$

Here ρ_w is the density of water, u_l the liquid water flow velocity and j_e the steam mass flux, given by $j_e = \frac{q_e}{H_v} = h_e(T - T_s)/H_v$, where H_v is the vaporisation enthalpy of water. Analogous to the heat transfer analysis this leads to the mass balance equation:

5 Modelling of material transport in a PWR primary circuit.

5.1 Outline of Material Transport Models.

(Figure 5-1) is a very simple schematic of a PWR primary circuit:

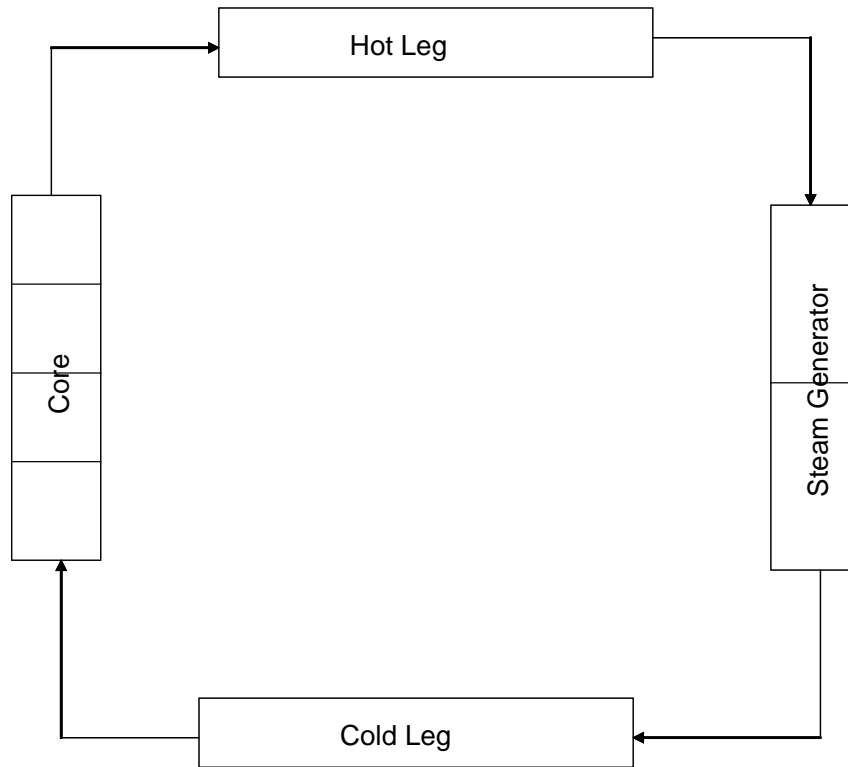


Figure 5-1: Simple schematic of PWR circuit.

As previously stated soluble and particulate Ni and Fe material are released from the cold leg, hot leg and steam generator and re-distributed around the circuit with the possibility of deposition in the core. To model this process the primary circuit can be split into N sections and, from molar conservation of either iron or nickel in solution around the primary circuit, the following equation applies

Equation 5-1:
$$V_i C_i \frac{dx_i}{dt} = \frac{\dot{m}}{\rho_{f,i-1}} C_{i-1} x_{i-1} - \frac{\dot{m}}{\rho_{f,i}} C_i x_i - J_i A_i \quad (i = 1 \dots N)$$

where V is the section volume, C is the total molar concentration of the coolant, x is the mole fraction of iron or nickel in the bulk coolant, ρ_f is the bulk density of water, \dot{m} is the mass flow rate, A is the section area, J is the molar flux of iron or nickel to the surface of the section, and suffix i denotes the plant section number. It is generally numerically more stable to formulate the problem in terms of mole fractions and this also makes it simpler to deal with changes in the fluid density. The steady state solution can be obtained by solving

Equation 5-2:
$$\frac{\dot{m}}{\rho_{f,i-1}} C_{i-1} x_{i-1} - \frac{\dot{m}}{\rho_{f,i}} C_i x_i - J_i A_i = 0$$

which is a set of non-linear equations and can be solved using any general method for solving such sets of equations.

6 Discussion and Summary

The problem of deposits on fuel cladding has been happening since the early PWR designs and is still occurring. Early occurrences were resolved by the introduction of better water chemistry, better operational procedures and material choices, but the requirement to operate existing plants at high powers and for longer fuel cycles meant a resurgence in the problem in the early to mid 90's. Even in the last decade several plants have experienced CIPS issues as a consequence of fuel crud, even though they operate with good water chemistry and use alloy 690 SG's.

Fuel crud arises from corrosion of out-of-core alloys, the release of a fraction of the corrosion products as soluble and particulate material and the re-deposition of this material in the core. Both deposition of soluble and particulate material is occurring, driven by the temperature gradient between the clad surface and bulk water and boiling enhanced mass transfer towards the surface. Precipitation on the clad surface is likely, the extent of which is driven by the degree of supersaturation of Ni. Particle deposition on the fuel clad also occurs and both processes are enhanced by boiling. Boiling increases the rate of deposition and moving from sub-cooled to wick boiling leads to a much greater fraction of the heat flux being removed by this mechanism. That is, the formation of crud leads to higher deposition rates in crud covered regions. This feed-back process can be mollified by a re-distribution of power in the fuel pin.

Once crud is formed conditions within these deposits can be very different than in the bulk coolant. Boric acid concentrations can be molar levels and Li concentrations are also very high. These large concentrations lead to significant increases in the saturation temperature of water and elevated temperatures with the crud. For crud thicknesses of 50 μ m or so temperature increases of the order of 10 degrees might be expected. Such temperature changes generally lead to a drop in the solubility limits of potential salts that can form in the crud and therefore their precipitation. Of particular concern are Li-Borate salts and in plants adding Zn then ZnO and Zn₂SiO₄ are potential precipitates. According to the models Li-Borate salts start to appear in crud around 20 μ m thick and this is consistent with the appearance of CIPS in plants. The increase in Li concentration in the crud could potentially increase clad corrosion rates, however such effects are mitigated by the presence of boric acid, also present. There has been no evidence that thick crud deposits lead to a significant increase in fuel failures in PWRs.

The processes of fuel crud formation and conditions within the crud can be modelled. This is not straightforward as all the differential equations required to describe the problem are coupled. The equations for material release, transport and deposition are also coupled to those for the fuel crud in two ways:

1. Deposition rates of soluble and particulate materials depend on the deposition boiling velocity. This term depends on the temperature profile through the crud, which depends on the thickness of crud, the increase in saturation temperature (dependent on coolant boric acid levels) and crud properties (porosity, chimney radius etc.).
2. Precipitation rates depend on species surface concentrations that depends on, T_o , the crud-coolant interface temperature. This term is determined by balancing conductive heat flux through the crud with the forced convective heat flux into the coolant. This balance equation depends on the heat transfer terms through the crud and therefore crud properties.

In general the models have been reasonably successful in predicting plant behaviour, both chemistry and neutronics observations. This is using reasonable, realistically physical, parameter values and using a consistent set of parameters across a range of PWR's. Probably the most uncertain term when performing calculations are the corrosion rates of out-of-core materials, as there are relatively wide ranges of these terms, based on measured data, some of which has been discussed here. However, there are still significant areas in which these models could be improved, for example the models for particle release and deposition are very simple, take no account of the particle size or local turbulence. Likewise, there is a large absence of important thermodynamic data with many equilibrium constants that are used having only been measured at low temperatures, compared to those expected in fuel crud. Both small scale laboratory studies and better plant measurements are required to improve these models.

Unit conversion

TEMPERATURE		
$^{\circ}\text{C} + 273.15 = \text{K}$	$^{\circ}\text{C} \times 1.8 + 32 = ^{\circ}\text{F}$	
T(K)	T($^{\circ}\text{C}$)	T($^{\circ}\text{F}$)
273	0	32
289	16	61
298	25	77
373	100	212
473	200	392
573	300	572
633	360	680
673	400	752
773	500	932
783	510	950
793	520	968
823	550	1022
833	560	1040
873	600	1112
878	605	1121
893	620	1148
923	650	1202
973	700	1292
1023	750	1382
1053	780	1436
1073	800	1472
1136	863	1585
1143	870	1598
1173	900	1652
1273	1000	1832
1343	1070	1958
1478	1204	2200

Radioactivity	
1 Sv	= 100 Rem
1 Ci	= 3.7×10^{10} Bq = 37 GBq
1 Bq	= 1 s^{-1}

MASS	
kg	lbs
0.454	1
1	2.20

DISTANCE	
x (μm)	x (mils)
0.6	0.02
1	0.04
5	0.20
10	0.39
20	0.79
25	0.98
25.4	1.00
100	3.94

PRESSURE		
bar	MPa	psi
1	0.1	14
10	1	142
70	7	995
70.4	7.04	1000
100	10	1421
130	13	1847
155	15.5	2203
704	70.4	10000
1000	100	14211

STRESS INTENSITY FACTOR	
MPa $\sqrt{\text{m}}$	ksi $\sqrt{\text{inch}}$
0.91	1
1	1.10